Stratification The formation of distinct layers with different densities (see 'pycnocline' above); stratification inhibits mixing or exchange between the nutrient-rich deeper water and the sunlit surface layer.
Subpolar gyres Large cyclonic water masses in the Northern Hemisphere between the subtropical front and the polar front.
Tropical Pertaining to the regions that, under the influence of the Trade Winds, are permanently stratified.
Upwelling Upward vertical movement of water into the surface mixed layer produced by divergence of the surface waters.
Zooplankton Animals that float or drift with ocean currents; microzooplankton are protozoan plankton that graze on small phytoplankton; mesozooplankton are crustaceans that graze on larger phytoplankton such as diatoms.

See also

Antarctic Circumpolar Current. California and Alaska Currents. Canary and Portugal Currents. Ekman Transport and Pumping. El Niño Southern Oscillation (ENSO). El Niño Southern Oscillation (ENSO) Models. Fisheries and Climate. Iron Fertilization. Microbial Loops. Network Analysis of Food Webs. Nitrogen Cycle. Ocean Color from Satellites. Ocean Gyre Ecosystems. Pacific Ocean Equatorial Currents. Pelagic Biogeography. Pelagic Fishes. Plankton. Plankton and Climate. Polar Ecosystems. Primary Production Distribution. Primary Production Processes. Redfield Ratio. Small Pelagic Species Fisheries. Somali Current.

Further Reading

Bakun A (1990) Global climate change and intensification of coastal ocean upwelling. *Science* 247: 198–201.
Barber RT and Chavez FP (1983) Biological consequences of El Niño. *Science* 222: 1203–1210.
Barber RT and Smith RL (1981) Coastal upwelling ecosystems. In: Longhurst A (ed.) *Analysis of Marine Ecosystems*, pp. 31–68. New York: Academic Press.
Longhurst A (1998) *Ecological Geography of the Sea*. San Diego: Academic Press.
Pauly D and Christensen V (1995) Primary production required to sustain global fisheries. *Nature* 374: 255–257.
Richards FA (ed.) (1981) *Coastal Upwelling*. Washington, DC: American Geophysical Union.
Ryther JH (1969) Photosynthesis and fish production in the sea. *Science* 166: 72–76.
Smith RL (1992) Coastal upwelling in the modern ocean. In: Summerhayes CP, Prell WL and Emeis K-C (eds) *Upwelling Systems: Evolution Since the Early Miocene*, Geological Society Special Publication 64, pp. 9–28. London: The Geological Society.
Summerhayes CP, Emeis, K-C, Angel MV, Smith RL and Zeitschel B (eds) *Upwelling in the Ocean Modern Processes and Ancient Records*. Chichester: Wiley.
Sverdrup HU (1955) The place of physical oceanography in oceanographic research. *Journal of Marine Research* 14: 287.

URANIUM–THORIUM DECAY SERIES IN THE OCEANS OVERVIEW

M. M. R. van der Loeff, Alfred-Wegener-Institut für Polar und Meeresforschung, Bremerhaven, Germany

doi:10.1006/rwos.2001.0168

Introduction

Natural radioactivity provides tracers in a wide range of characteristic timescales and reactivities, which can be used as tools to study the rate of reaction and transport processes in the ocean. Apart from cosmogenic nuclides and the long-lived radioisotope K-40, the natural radioactivity in the ocean is primarily derived from the decay series of three radionuclides that were produced in the period of nucleosynthesis preceding the birth of our solar system: Uranium-238, Thorium-232, and Uranium-235 (a fourth series, including Uranium-233, has already decayed away). The remaining activity of these so-called primordial nuclides in the Earth's crust, and the range of half-lives and reactivities of the elements in their decay schemes, control the present distribution of U-series nuclides in the ocean.

The Distribution of Radionuclides of the Uranium Thorium Series in the Ocean

Distribution of ^{238}U, ^{235}U, ^{234}U, and ^{232}Th (*see* Uranium–Thorium Series Isotopes in Ocean Profiles)

Uranium is supplied to the ocean by rivers. In sea water it is stabilized by a strong complexation as

uranyl carbonate $UO_2(CO_3)_3^{4-}$, causing its long residence time in the ocean. U follows closely the distribution of salinity with ^{238}U (in $dpm\,l^{-1}$) = 0.0704* salinity. (Note: dpm = disintegrations per minute. The SI Unit Bq, 60 dpm = 1 Bq, is not used in the literature on natural radioactivity in the ocean.) Under anoxic conditions, U is reduced from the soluble (VI) to the insoluble (IV) oxidation state and rapidly removed from sea water. Reductive removal occurs especially in sediments underlying high productivity or low-oxygen bottom waters. Locally this may influence the U–salinity relationship. Salinity-corrected U contents have a variation of 3.8% in the world ocean and are about 1% higher in the Pacific than in the Atlantic Ocean. At lower salinities in estuaries, salinity-corrected U contents are much more variable as a result of removal and release processes and of interaction with organic complexants and colloids.

^{235}U is chemically equivalent to ^{238}U and occurs with a $^{235}U/^{238}U$ activity ratio of 0.046. As a result of the preferential mobilization of ^{234}U during chemical weathering, the river supply of ^{234}U activity exceeds the supply of ^{238}U, causing a $^{234}U/^{238}U$ ratio in the ocean greater than unity. The isotopic composition of uranium in sea water with salinity 35 is shown in **Table 1**.

Like U, ^{232}Th is a component of the Earth's crust and is present in the lithogenic fraction of every marine sediment. As a result of its high particle reactivity, Th is rapidly removed from the water column. The ^{232}Th activity in the ocean is very low (around $3 \times 10^{-5}\,dpm\,l^{-1}$ or 0.1 ng/kg) and its distribution can be compared to that of other particle-reactive elements like Al or Fe.

Distribution of Isotopes from the Three Decay Series

In all three decay series, isotopes of relatively soluble elements like U, Ra, and Rn, decay to isotopes of highly particle-reactive elements (Th, Pa, Po, Pb), and vice versa (**Figure 1**), resulting in widely different distributions in the water column (**Table 2**) (*see* **Uranium–Thorium Series Isotopes in Ocean Profiles**).

Table 1 Average isotopic uranium composition of sea water with salinity 35

Parameter	*Value*
$^{235}U + ^{238}U$ concentration	$3.238\,ng\,g^{-1}$
$^{235}U/^{238}U$ activity ratio	0.0460
$^{234}U/^{238}U$ activity ratio	1.144 ± 0.002
Isotope activity	
^{238}U	$2.46\,dpm\,l^{-1}$
^{234}U	$2.82\,dpm\,l^{-1}$
^{235}U	$0.113\,dpm\,l^{-1}$

In a closed system, given enough time, all nuclides in a decay series reach secular equilibrium. This means that growth is balanced by decay, and that all intermediate nuclides have the same activity. In a natural open system, however, reaction and transport cause a separation between parent and daughter nuclides. The resulting disequilibria between parent and daughter nuclide can be used to calculate the rate of the responsible processes.

Disequilibrium: The Basis for Flux Calculations (Figure 2)

Mobile Parent with Particle-reactive Daughter (Table 3)

Tracers in this group are produced in the water column and removed on sinking particles, a process called scavenging. They allow us to determine particle transport rates in the ocean.

In a simple box model the total daughter activity (A_D^t) is determined by decay (decay constant $\lambda = \ln(2)/t_{1/2}$), ingrowth from the parent nuclide (activity A_p, production rate of daughter nuclide $P_D = \lambda A_p$) and removal on sinking particles J (**Figure 3**):

$$\frac{dA_D^t}{dt} = P_D - \lambda A_D^t - J = \lambda(A_P - A_D^t) - J \qquad [1]$$

In steady-state the flux is directly related to the depletion of the daughter with respect to the parent:

$$J = \lambda(A_P - A_D^t) \qquad [2]$$

and the residence time of the daughter nuclide with respect to scavenging, τ_{sc}, is given by the quotient of activity and removal rate:

$$\tau_{sc} = \frac{A_D^t}{J} = \frac{A_D^t}{\lambda(A_P - A_D^t)} \qquad [3]$$

Elements in this group are described below.

Thorium ^{230}Th is produced at a known rate from ^{234}U in sea water. The highly reactive element is rapidly adsorbed onto particles and transported down in the water column when these particles sink out. As the adsorption is reversible, a steady-state distribution is achieved, in which both particulate and dissolved activities increase linearly with depth

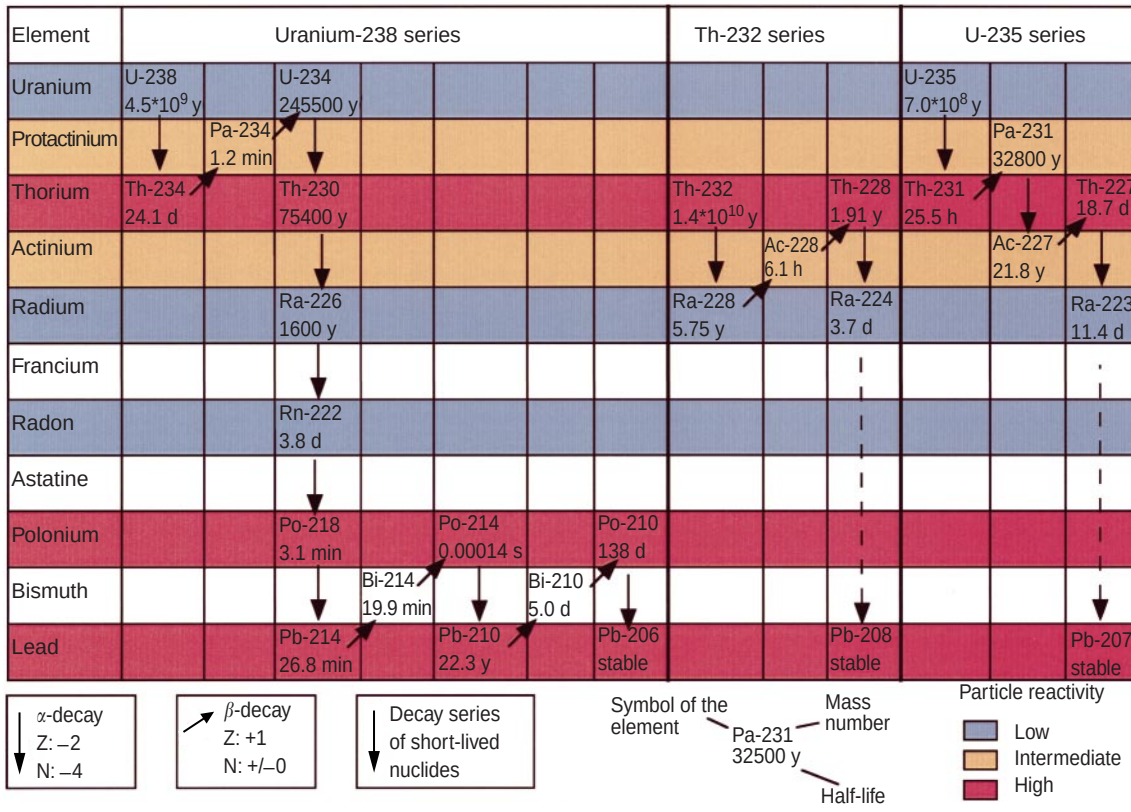

Figure 1 The natural uranium-thorium decay series, colored according to particle reactivity. The arrows represent decay with the changes in atomic number (Z) and number of nucleons (N) indicated. All three series end with a stable lead isotope.

(*see* **Uranium–Thorium Series Isotopes in Ocean Profiles**). At any depth, disregarding horizontal advection, the vertical flux of $^{230}Th_{xs}$ ('xs' meaning in excess of the activity supported by the parent nuclide, in this case the small amount of ^{234}U on the sinking particles) must equal its production from ^{234}U in the overlying water column (depth z in meters), which amounts to:

$$P_{230} = \lambda_{230} A_{234} z = 9.19 \times 10^{-6} (y^{-1}) \; 2820 \; (dpm\, m^{-3}) z(m) = 0.0259\, z\, (dpm\, m^{-2}\, y^{-1}) \quad [4]$$

This known, constant ^{230}Th flux, depending only on water depth, is a powerful tool to quantify errors in the determination of rain rates of other components of the particle flux, either by sediment traps or through the accumulation rate of a marine sediment. The collection efficiency of sediment traps, known to be highly variable and dependent on trap design, turbulence, and flow rates, can be derived from a comparison of the intercepted ^{230}Th flux F_{230} with the theoretical flux P_{230} (see below for a refinement of this procedure using ^{231}Pa). The vertical rain rate R_i of any component i of the particle flux can be derived from the ratio of the concentration C_i to the ^{230}Th activity in the particles A_{230}, using:

$$R_i = \frac{C_i}{A_{230}} P_{230} \quad [5]$$

Table 2 List of the elements (with isotopes of half-life $t_{1/2} > 1$ day) in the U decay series with their scavenging residence time in deep and surface ocean and their estimated particle-water partition coefficient K_d, showing the relative mobility of U, Ra, and Rn

Element	*Scavenging residence time (years)*		K_d ($cm^3\, g^{-1}$)
	Deep sea	*Surface ocean*	
U	450 000		500
Pa	130	< 1	1×10^6
Th	30	< 1	1×10^7
Ac	decays (> 30)		$0.4–2 \times 10^5$
Ra	1000		$0.2–3 \times 10^4$
Rn	decays	gas exchange with atmosphere	0
Pb	50–100	2	1×10^7
Po	decays (> 2)	0.6	2×10^7

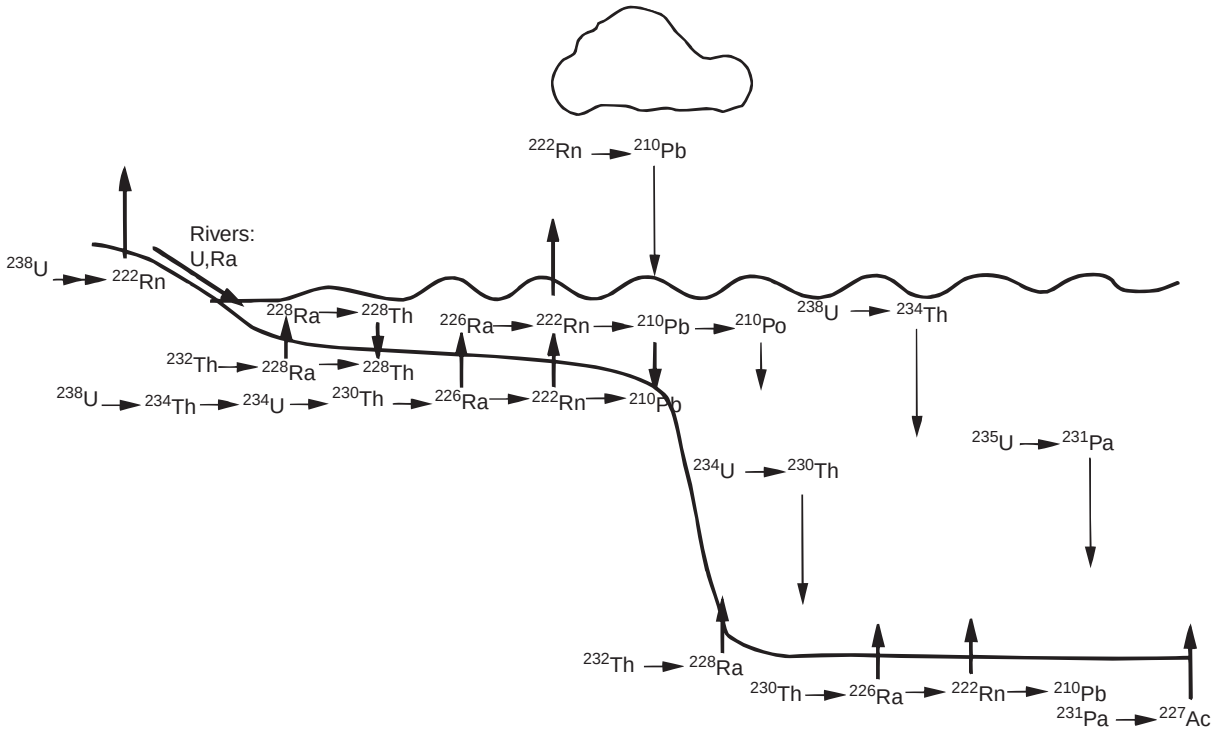

Figure 2 Schematic diagram of radioactive decay (horizontal arrows) and typical transport processes in ocean and atmosphere that can be traced by the nuclides described here (vertical arrows). (Adapted with permission from Ernst WG and Morin JG (eds) 1980 *The Environment of the Deep Sea.* Englewood Cliffs, NJ: Prentice Hall.)

In a similar way, the past flux of $^{230}Th_{xs}$ to the sea floor, $^{0}F_{230}$, derived from decay-corrected ^{230}Th activities ($^{0}A_{230}$) in dated sediment core sections, can be compared to the theoretical rain rate. The ratio $\Psi = {}^{0}F_{230}/P_{230}$, the focusing factor, is used to determine to what extent the sediment core location has been subject to focusing or winnowing during certain geological periods. The preserved vertical rain rate of sediment components corrected for such redistribution effects follows in analogy to eqn [5]:

$$R_i = \frac{C_i}{{}^{0}A_{230}} P_{230} \qquad [6]$$

^{234}Th is produced from the decay of ^{238}U in sea water. In the deep ocean, approximately 3% of its activity is on particles and removal is so slow compared with its half-life (24.1 days) that total (dissolved + particulate) ^{234}Th is in secular equilibrium with ^{238}U. In coastal and productive surface waters, however, scavenging (**Figure 3**) causes a strong depletion of ^{234}Th (**Figure 4**). Following eqn [2], the depth-integrated depletion in the surface water yields the export flux of ^{234}Th. If required, the calculation can be refined to include advection and non-steady-state situations. The resulting flux of ^{234}Th out of the surface layer of the ocean is the most

Table 3 Isotope pairs with mobile parents and particle-reactive daughters

Mother	*Daughter*	*Half-life*	*Source*	*Oceanographic applications*
^{234}U	^{230}Th	75200 y	water column	sediment trap calibration, reconstruction of past vertical rain, sediment focusing
^{238}U	^{234}Th	24.1 d	water column	export production, calibration of shallow sediment trap resuspension budgets, bioturbation
^{228}Ra	^{228}Th	1.9 y	water column, in deep sea and continental shelf	scavenging in coastal waters, bioturbation
^{235}U	^{231}Pa	32500 y	water column	boundary scavenging, paleoproductivity, refined sediment trap calibration
^{226}Ra	^{210}Pb	22.3 y	water column, atmosphere	boundary scavenging, bioturbation
^{210}Pb	^{210}Po	138 d	water column	scavenging in surface ocean

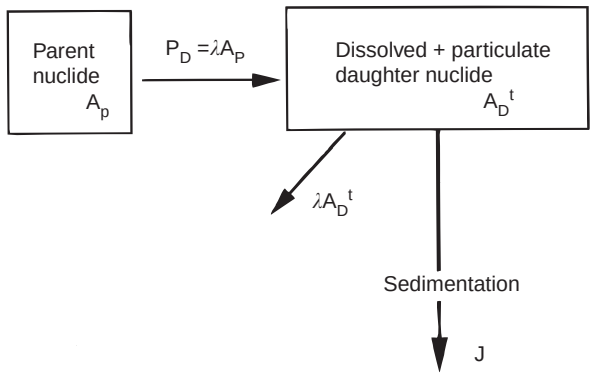

Figure 3 Schematic diagram of the scavenging of a particle-reactive daughter nuclide (decay constant λ) produced in the water column from a soluble parent.

suitable way to calibrate shallow sediment traps. The export flux of other constituents, like organic carbon or biogenic silica, can be derived from the export flux of ^{234}Th if the ratio of these constituents to particulate ^{234}Th in the vertical flux is known. This ratio is variable and depends, for example, on particle size, and the uncertainty in the determination of this ratio limits the quality of ^{234}Th-based estimates of export production from the upper ocean.

A very similar situation exists near the seafloor, where resuspended sediment particles scavenge ^{234}Th from the bottom water. The resulting depletion of ^{234}Th in the benthic nepheloid layer (BNL) is a measure of the intensity of the resuspension-sedimentation cycle on a timescale of weeks. The tracer thus shows whether a nepheloid layer is advected over large distances or sustained by local resuspension.

Mass balance requires that the activity removed from surface waters and from the BNL is balanced by excess activities below (i.e. activities in excess of the activities supported by ^{238}U). Excess activities have sometimes been observed in mineralization horizons in the water column below the euphotic zone and are common in the surface sediment. The distribution of excess ^{234}Th in the sediment is used to calculate bioturbation rates on short timescales.

The half-life of 1.9 years makes ^{228}Th useful as a tracer for particle flux on a seasonal or interannual timescale. However, due to the highly inhomogeneous distribution of its parent ^{228}Ra, the interpretation is much more complicated than in the case of ^{234}Th, for example.

As regards multiple Th isotopes as an in situ coagulometer, it has been shown that Th isotopes in the ocean are in reversible exchange between the particulate and dissolved form (**Figure 5**) and in steady-state, including radioactive decay we have:

$$\frac{A^{part}}{A^{diss}} = \frac{k_1}{\lambda + k_{-1}} \qquad [7]$$

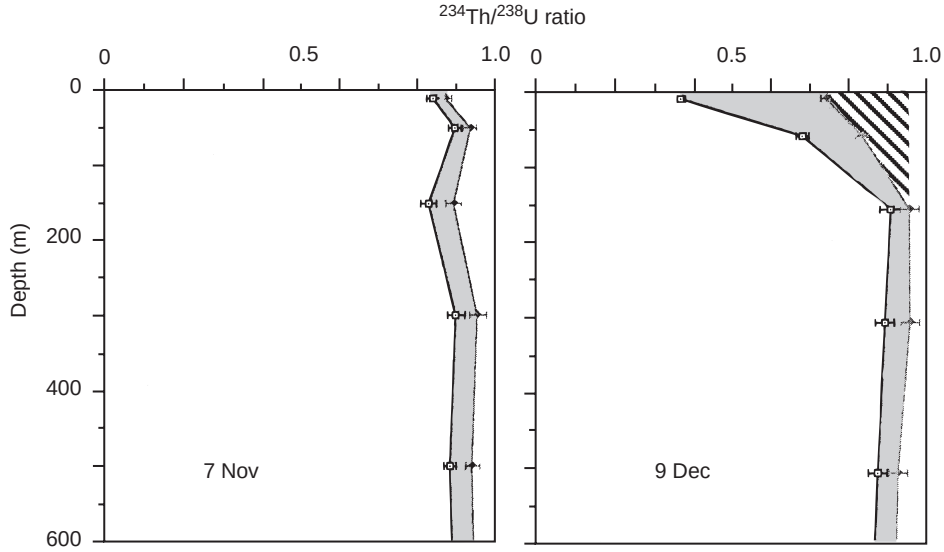

Figure 4 ^{234}Th : ^{238}U ratio before (left) and during (right) a plankton bloom in the Bransfield Strait, Antarctic Peninsula. The left profile in each diagram represents dissolved, the right profile total ^{234}Th activities. More ^{234}Th was adsorbed to particles (shaded) in the bloom. Total ^{234}Th was probably in equilibrium with ^{238}U in November, but became depleted in the surface water in December (hatched) due to particle export. (Adapted from Scavenging and particle flux: seasonal and regional variations in the Southern Ocean (Atlandic sector). *Marine Chemistry* 35, Rutgers van der Loeff and Berger, 553–567, Copyright (1991) with permission from Elsevier.)

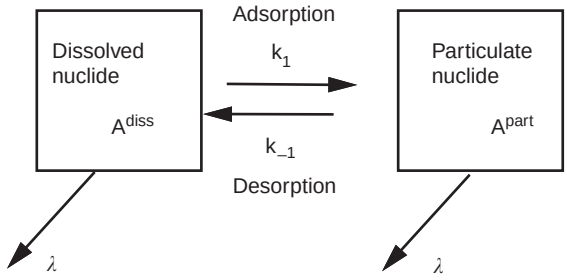

Figure 5 Box model of the reversible exchange between the dissolved and particulate form of a nuclide with adsorption and desorption rate constants k_1 and k_{-1}.

where A^{part} and A^{diss} are the particulate and dissolved activities, k_1 is the desorption rate constants. If the distribution of two or more isotopes (usually ^{234}Th and ^{230}Th or ^{228}Th and ^{234}Th) between dissolved and particulate forms is known, k_1 and k_{-1} can be calculated. Values for $1/k_1$ derived for thorium are on the order of a month in bloom situations and >1 year in clear deep water, much longer than expected from adsorption theory. This is explained when thorium adsorbs to colloidal-sized particules and the rate limiting steps, which determine the distribution of the tracers over dissolved and filterable form, are the coagulation and disaggregation with rate constants k_2 and k_{-2} respectively (**Figure 6**). Thus, when aggregation is clearly slower than adsorption ($k_2 \ll k_1$) thorium isotopes provide a way to derive particle aggregation rates *in situ*.

Protactinium ^{231}Pa is produced from the decay of ^{235}U in sea water. The behavior of ^{231}Pa is very similar to that of ^{230}Th, and these two uranium daughters are produced throughout the water column in a constant activity ratio, given by the production rate of ^{231}Pa divided by the production rate of ^{230}Th or $A_{235}\lambda_{231}/A_{234}\lambda_{230} = 0.093$. The major application of ^{231}Pa lies in the combined use of these two tracers, whose exact production ratio is known. The approximately 10 times lower reactivity of ^{231}Pa allows it to be transported laterally over larger distances than ^{230}Th before being scavenged. The resulting basin-wide fractionation between ^{231}Pa and ^{230}Th is the basis for the use of the ^{231}Pa/^{230}Th ratio as a tracer of productivity. In areas of high particle flux the particles have a ^{231}Pa/^{230}Th ratio >0.093, whereas particles sinking in low productivity gyres have a ratio <0.093. The ^{231}Pa/^{230}Th ratio stored in the sediment, after proper correction for decay since deposition, is a powerful tool for the reconstruction of paleoproductivity. The fractionation between Th and Pa depends on particle composition and has been found to be much lower when opal is abundant. The tracer loses much of its value in a diatom-dominated system like the Southern Ocean.

A related application of the ^{231}Pa/^{230}Th ratio is a correction to the ^{230}Th-based calibration of sediment trap efficiency. The removal of both nuclides from sea water can be divided into a vertically scavenged component (V_{230}; V_{231}) and a component transported horizontally by eddy mixing or advection (H_{230}; H_{231}) (**Figure 7**).

$$P_{230} = V_{230} + H_{230} \quad [8]$$

$$P_{231} = V_{231} + H_{231} \quad [9]$$

The calibration of sediment traps is based on the comparison of the intercepted ^{230}Th flux F_{230} with the predicted vertical flux V_{230}. In the original ^{230}Th-based calibration procedure (eqn [4]), H_{230} is

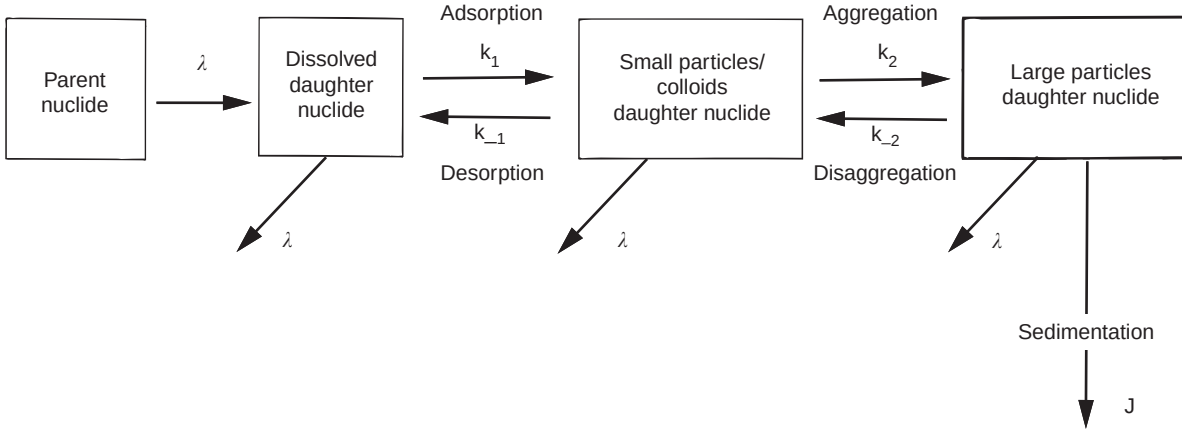

Figure 6 Conceptual model, including the models depicted in **Figures 3** and **5**, of the processes thought to control scavenging of radionuclides. (Adapted from Seasonality in the flux of natural radionuclides and plutonium in the deep Sargasso Sea. *Deep-Sea Research* 32, Bacon MP *et al.,* 273–286, Copyright 1985 with permission from Elsevier Science.)

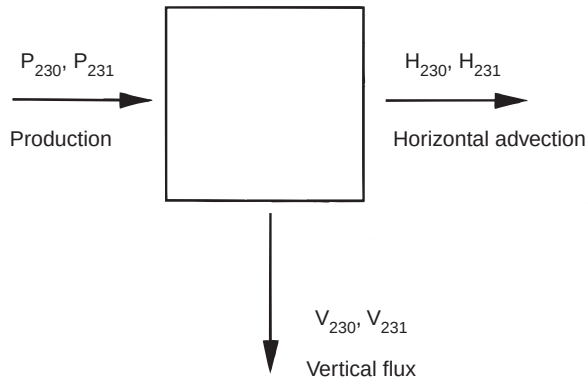

Figure 7 Box model used to derive the vertical flux of ^{230}Th.

neglected and F_{230} is compared directly to the production rate P_{230}. Since P_{230} (eqn [4]) and P_{231} are known and the V_{230}/V_{231} ratio can be measured as the $^{230}Th_{xs}/^{231}Pa_{xs}$ ratio in the sediment trap material, it is sufficient to estimate the H_{230}/H_{231} ratio from water column distributions to solve eqns [8] and [9] for V_{230} and obtain a refined estimate of trapping efficiency.

Lead ^{210}Pb (half-life 22.3 years) is produced from ^{222}Rn, the immediate daughter of ^{226}Ra. ^{222}Rn emanation from land is the major source of ^{210}Pb deposition from the atmosphere (**Figure 2**). ^{222}Rn emanation from surface sea water accounts for only 2% of ^{222}Rn in the atmosphere, but is a significant source in remote areas like the Antarctic Ocean. Below the surface water, seawater ^{226}Ra becomes the most important source.

The high particle reactivity makes ^{210}Pb a tracer for particle flux. This is shown most clearly by the good correlation between the fluxes of ^{210}Pb and of biogenic material in sediment traps. Thus, low ^{210}Pb activities (or ^{210}Pb/^{226}Ra ratios) in surface and deep water, high ^{210}Pb fluxes in traps, and high inventories in the sediment all point to high particle fluxes and consequently high productivity. (Note, however, that in hemipelagic sediments in productive ocean areas the redox cycling of Mn can cause additional near-bottom scavenging of Pb.) Due to this removal on biogenic particles, ^{210}Pb shows strong boundary scavenging similar to ^{231}Pa, with accumulation rates in the sediments of productive (especially eastern) ocean boundaries that are far above local production and atmospheric deposition, whereas the flux to deep-sea sediments in oligotrophic central gyre regions can be very low. Consequently, the flux of ^{210}Pb into and its inventory in surface sediments is highly variable in space. But as long as the (yearly averaged) scavenging conditions do not change with time, the ^{210}Pb flux to the sediment at a certain location can be considered constant, a prerequisite for the interpretation of ^{210}Pb profiles to derive sedimentation and bioturbation rates.

Due to the relatively well-known production and input rates of ^{210}Pb, the scavenging residence time τ_{sc} can be derived from the distribution of ^{210}Pb in the ocean (compare eqn [3]). τ_{sc} was found to increase from about 2 years in the surface ocean to about 35 years in the deep Atlantic and 150 years in the deep Pacific, a result that is used to understand the behavior of stable lead. This illustrates how ^{210}Pb is a useful analog for stable lead, the study of which is complicated by the extreme risk of contamination (*see* **Anthropogenic Trace Elements in the Ocean**).

Polonium ^{210}Po, the immediate daughter of ^{210}Pb, is highly particle-reactive. The 138-day half-life of ^{210}Po makes the ^{210}Po/^{210}Pb tracer pair a suitable extension to ^{234}Th as tracer for seasonal particle flux from the surface ocean. The non-homogeneous distribution and reactivity of the parent ^{210}Pb implies that ^{210}Po can only be used if concurrent accurate measurements are made of ^{210}Pb.

As a result of the strong affinity for organic material and cytoplasm, ^{210}Po accumulates in the food chain and ^{210}Po/^{210}Pb activity ratios from around 3 in phytoplankton to around 12 in zooplankton have been reported. A high excess ^{210}Po activity is therefore indicative of a pathway including zooplankton. The preference of Po for organic material in comparison with Pb and Th, which may adsorb on any surface, can be exploited to distinguish between the fluxes of organic carbon and other components of the particle flux.

Reactive Parent with Mobile Daughter (Table 4)

This type of tracer is used to quantify diffusion, advection, and mixing rates of water masses, for example, the distribution of ^{222}Rn near the seafloor. The parent, ^{226}Ra, has a far higher activity in marine sediments (^{222}Rn emanation rate A^s_{226} of order $100\,\mathrm{dpm\,l^{-1}}$ wet sediment) than in the bottom water (A^w_{226} of order $0.2\,\mathrm{dpm\,l^{-1}}$). This gradient causes a diffusion of the daughter ^{222}Rn from the sediment into the water column, and a typical vertical distribution as shown in **Figure 8**.

The distribution of ^{222}Rn, A_{222}, can be described by the diffusion-reaction equation:

$$\frac{dA_{222}}{dt} = \lambda(A_{226} - A_{222}) + D\frac{d^2A_{222}}{dz^2} \qquad [12]$$

Table 4 Isotope pairs with a particle-reactive parent and a mobile daughter

Mother	*Daughter*	*Half-life*	*Source*	*Oceanographic application*
^{231}Pa	^{227}Ac	22 y	deep-sea sediments	ocean circulation, upwelling
^{232}Th	^{228}Ra	5.8 y	all terrigenous sediments	tracing of shelf water sources, mixing in deep-sea and surface water
^{230}Th	^{226}Ra	1600 y	deep-sea sediments	ocean circulation, ground-water inputs
^{228}Th	^{224}Ra	3.6 d	^{232}Th (sediment) ^{228}Ra (sediment + water column)	mixing in shelf waters and estuaries
^{227}Th	^{223}Ra	11.4 d	^{235}U (sediment) ^{231}Pa (sediment + water column)	mixing in shelf waters and estuaries
^{226}Ra	^{222}Rn	3.8 d	(deep-sea) sediments	mixing in bottom water, air–sea gas exchange, ground-water inputs

where D is the diffusion coefficient. This yields in steady state:

$$A_{222} = A_{226} - (A^{o}_{222} - A_{226})e^{-\sqrt{(\lambda/D)}z} \qquad [13]$$

A solution valid for the sediment and the water column (if z is defined positive as the distance to the interface), where A^{o}_{222} signifies the ^{222}Rn activity at the interface (**Figure 8**). In the sediment, this corresponds to an integrated depletion of:

$$I_s = (A^{s}_{226} - A^{0}_{222})\sqrt{\frac{D}{\lambda}} \qquad [14]$$

maintained by a ^{222}Rn release rate of:

$$F_s = \lambda I_s \qquad [15]$$

In the water column, this flux causes an excess activity which is transported upwards by turbulent diffusion (coefficient K). The integrated ^{222}Rn excess in the bottom water is given by:

$$I_w = (A^{0}_{222} - A^{w}_{226})\sqrt{\frac{K}{\lambda}} \qquad [16]$$

maintained by a supply from the sediment

$$F_w = \lambda I_w \qquad [17]$$

Note that mass balance requires that $F_s = F_w$ and that the depletion in the sediment equals the excess in the water column ($I_s = I_w$). The example shows how the diffusion coefficient in the sediment and the vertical eddy diffusion coefficient in the bottom water can be derived from measurements of the vertical distribution of this tracer using eqn [13].

Elements in this group are described below.

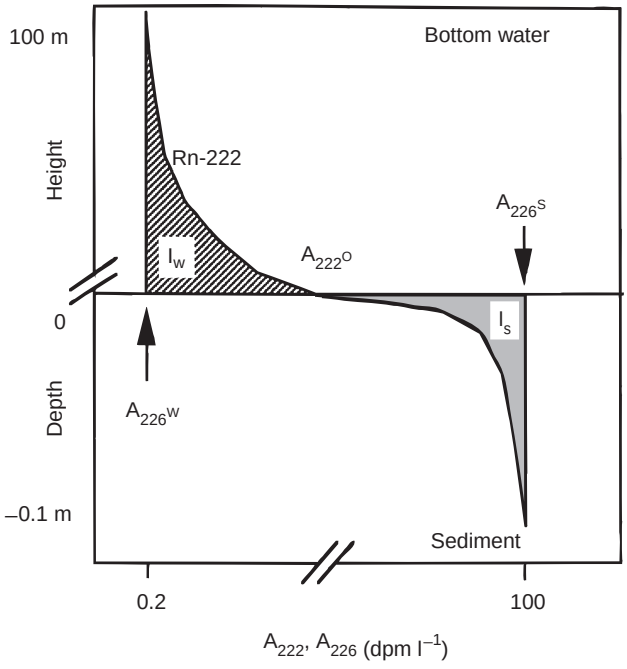

Figure 8 Generalized distribution of ^{226}Ra and ^{222}Rn in surface sediments and bottom water (note change in horizontal and vertical scales). The cumulative ^{222}Rn depletion in the sediment (I_s, shaded) is balanced by the ^{222}Rn excess in the bottom water (I_w, hatched). The vertical extent of the disequilibrium is 3 orders of magnitude larger in the water column than in the sediment, corresponding to the 6 orders of magnitude difference in diffusion coefficient (on the order of 10 $cm^2 s^{-1}$ in the bottom water as opposed to 10^{-5} cm^2 s^{-1} in the sediment).

Actinium ^{227}Ac is produced by the decay of ^{231}Pa. Over 99% of ^{231}Pa produced in the water column resides in the sediment, with highest specific activities in slowly accumulating deep-sea sediments. As actinium is relatively mobile, it is released to the pore water and from there to the overlying water, very similar to the behavior of ^{226}Ra and ^{228}Ra. This

results in a strong signal from the deep seafloor on top of a background concentration, which is given by the distribution of ^{231}Pa in the ocean. The nuclide is therefore a potential tracer for vertical mixing and advection (e.g. upwelling) on a decennium timescale.

Radium Radium is relatively mobile and the major source of the isotope ^{226}Ra is the production from the ^{230}Th in the upper layer of sediments. Just like ^{227}Ac, this source is strongest over deep-sea sediments with a slow accumulation rate. The intermediate reactivity of radium (**Table 2**) and its half-life (1600 years) in the order of the ocean mixing time (around 1000 years) explain its distribution as a 'biointermediate' element: ^{226}Ra activities are low in surface waters but never become depleted. They increase with depth and with the age of water masses in the conveyor-belt circulation to reach highest values in the deep north Pacific around 340 dpm m^{-3}. Extensive attempts in the GEOSECS program to use the isotope as a tracer of ocean circulation and water mass age proved unsuccessful as a result of the diffuse nature of the source. Even a normalization with barium, an element that can to a certain extent be regarded as a stable analog of radium, could not sufficiently account for this variation.

Ground waters sometimes have high ^{226}Ra activities. The isotope can then be used to trace ground-water inputs to the coastal ocean.

^{228}Ra is also produced in marine sediments, but in contrast to ^{226}Ra and ^{227}Ac, its parent ^{232}Th is present in the terrigenous fraction of all sediments irrespective of water depth. In combination with the relatively short half-life (5.8 years), this results in a distribution in the open ocean with enhanced concentrations near the seafloor of the deep ocean and near the continental slope, while the activities can accumulate to highest values over extensive continental shelf areas. The vertical distribution in the deep sea (**Figure 9**) resembles the exponential decay that would be expected in a one-dimensional (1-D) model with the source in the seafloor, vertical mixing, and radioactive decay (eqn [13]). This would allow the tracer to be used to derive the vertical mixing rate in the deep ocean. However, it has been shown that even in a large ocean basin like the north-east Atlantic, horizontal mixing is so strong that the vertical distribution is influenced by inputs from slope sediments, making the 1-D model inadequate.

The inputs of shelf waters to the open ocean cause the high activities in the surface waters, illustrated by a typical profile in **Figure 9**. This surface water signal has a strong gradient from the continental shelf to the inner ocean, which has been used to derive horizontal eddy diffusion coefficients in a way analogous to eqn [13]. As the distribution of ^{228}Ra has been shown to vary with time, a steady-state distribution can usually not be assumed, and a repeated sampling is required. Moreover, the horizontal distribution is affected by advection and vertical diffusion, making the interpretation rather complicated. The combination of various radium isotopes (see below), can alleviate some of these problems.

In surface current systems away from the continents, ^{228}Ra becomes a powerful tracer for waters that have been in contact with the continental shelf. The ^{228}Ra enrichment in surface waters in the equatorial Pacific point to shelf sources off New Guinea, from where the isotope is carried eastward in the North Equatorial Counter Current. In this plume, the vertical distribution of the isotope has been used to derive vertical mixing rates. A very high accumulation of ^{228}Ra is observed in the transpolar drift in the central Arctic Ocean, a signal derived from the extensive Siberian shelves.

Due to their short half lives, ^{224}Ra (3.4 days) and ^{223}Ra (11.4 days) are interesting only in the immediate vicinity of their sources. In the open ocean they are close to secular equilibrium with their parents ^{228}Th and ^{227}Ac, but in coastal waters these tracers are being developed to study mixing rates. Their distribution is controlled here by sources in the estuary and on the shelf, mixing and decay. Horizontal mixing rates have been obtained from the distribution of ^{223}Ra and ^{224}Ra across the shelf using eqn [13]. As with ^{228}Ra, this procedure is limited to cases where the mixing can be considered to be one-dimensional, but the steady-state requirement is more easily met at these short timescales. The ^{223}Ra/^{224}Ra activity ratio, which decays with a half-life of 5.4 days, yields the age of a water mass since its contact with the source, irrespective of the nature of the mixing process with offshore waters.

Radon With its half-life of 3.8 days, the readily soluble gas ^{222}Rn is in secular equilibrium with its parent ^{226}Ra in the interior ocean. At the boundaries of the ocean, however, inputs from sediments and release to the atmosphere create concentration gradients carrying useful kinetic information. The distribution of excess ^{222}Rn near the seafloor is used to quantify vertical diffusion (see above, **Figure 8**) and ground-water inputs; the depletion of ^{222}Rn in surface waters has been used to quantify the air–sea gas exchange rate.

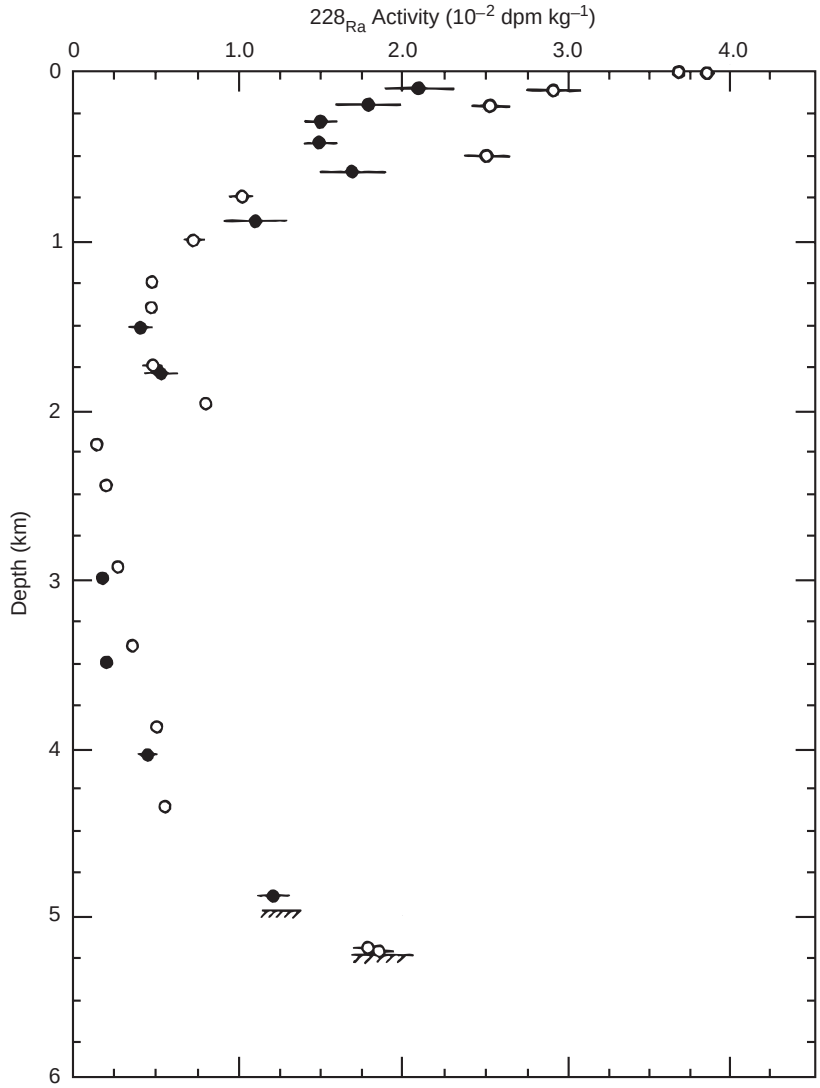

Figure 9 Typical ^{228}Ra activity profiles in the water column in the North Atlantic, showing the enrichment near the seafloor and in the surface water. (Adapted with permission from Ivanovich M and Harmon RS (eds) 1992 *Uranium-series Disequilibrium*, 2nd edn).

Summary

The accurate clocks provided by the uranium-thorium decay series enable us to extract rate information from the measurement of radioactive disequilibria in the ocean. Among the wide spectrum of available tracers, a mother–daughter pair with appropriate reactivities and half-lives can be found for a multitude of processes related to particle transport, water mass transport and mixing, and gas exchange (**Table 5**).

Glossary

A^{diss}	dissolved activity
A_P	parent activity
A^{part}	particulate activity
A_{222}	^{222}Rn activity
A^{o}_{222}	^{222}Rn activity at sediment–water interface
A_{226}	^{226}Ra activity
A^{w}_{226}	^{226}Ra activity in the bottom water
A^{s}_{226}	radon emanation rate in sediment
A_{230}	^{230}Th activity in the particles
A_{234}	activity of ^{234}U
$^{0}A_{230}$	decay-corrected ^{230}Th activities
A_{235}	^{235}U activity
A^{t}_{D}	total daughter activity
C_i	concentration of component i
D	diffusion coefficient
F_s	^{222}Rn release rate
F_w	^{222}Rn input rate

F_{230}	intercepted ^{230}Th flux
$^{0}F_{230}$	past flux of $^{230}Th_{xs}$ to the seafloor
H_{230}	horizontal flux of ^{230}Th
H_{231}	horizontal flux of ^{231}Pa
I_s	^{222}Rn depletion in the sediment
I_w	^{222}Rn excess in the bottom water
J	sedimentaion rate
K	turbulent diffusion coefficient
K_d	particle-water partition coefficient
λ	decay constant
k_1	adsorption rate constant
k_{-1}	desorption rate constant
k_2	coagulation rate constant
k_{-2}	disaggregation rate constant
N	number of nucleons
P_D	production rate
P_{230}	production rate of ^{230}Th
$^{231}Pa_{xs}$	excess activity of ^{231}Pa
P_{231}	production rate of ^{231}Pa
t	time
$t_{1/2}$	half-life
$^{230}Th_{xs}$	excess activity of ^{230}Th
R_i	rain rate of component i
V_{230}	vertical flux of ^{230}Th
V_{231}	vertical flux of ^{231}Pa
z	depth
Z	atomic number
λ_{230}	decay constant of ^{230}Th
λ_{231}	decay constant of ^{231}Pa
τ_{sc}	scavenging residence time
Ψ	focusing factor

See also

Air–Sea Gas Exchange. Anthropogenic Trace Elements in the Ocean. Dispersion and Diffusion in the Deep Ocean. Hydrothermal Vent Fluids, Chemistry of. Nepheloid Layers. Ocean Margin Sediments. Sediment Chronologies. Sedimentary Record, Reconstruction of Productivity from the. Tracers of Ocean Productivity. Uranium–Thorium Series Isotopes in Ocean Profiles.

Table 5 Summary of the processes that can be investigated using the natural uranium-thorium decay series

Processes	*Tracers*
Particle fluxes	
Boundary scavenging	$^{231}Pa/^{230}Th$, ^{210}Pb
(Paleo) productivity	$^{231}Pa/^{230}Th$, ^{210}Pb
Export production	^{234}Th
Scavenging, trace metal behavior	^{234}Th, ^{230}Th, ^{210}Pb, ^{210}Po
Sediment trap efficiencies	^{234}Th, ^{230}Th, ^{231}Pa
Aggregation rates of particles and colloids	Joint Th isotopes
Sediment redistribution in bottom water	^{230}Th
Resuspension near seafloor	^{234}Th, ^{210}Pb
Water masses	
Shelf interaction/horizontal mixing rates	^{228}Ra, ^{224}Ra, ^{223}Ra
Vertical mixing rates	^{222}Rn, ^{228}Ra, ^{227}Ac
Upwelling	^{227}Ac
Ground-water inputs	^{226}Ra, ^{222}Rn
Gas exchange	
Exchange with atmosphere	^{222}Rn

Further Reading

Bacon MP and Anderson RF (1982) Distribution of thorium isotopes between dissolved and particulate forms in the deep sea. *Journal of Geophysical Research* 87: 2045–2056.

Broecker WS and Peng T-H (1982) *Tracers in the Sea*. Columbia University, New York: Lamont-Doherty Geological Observatory. Eldigio Press.

Cochran JK (1992) The oceanic chemistry of the Uranium and Thorium-series nuclides. In: Ivanovich M and Harmon RS (eds) *Uranium-series Disequilibrium: Applications to Earth, Marine, and Environmental Sciences*, 2nd edn, pp. 334–395. Oxford: Clarendon Press.

Firestone RB (1998) *Table of Isotopes*, 8th edn. In: Baglin CM (ed) and Chu SYF (CD-ROM ed) New York: Wiley.

Grasshoff K, Kremling K and Ehrhardt M (1999) *Methods of Seawater Analysis*, 3rd edn, pp. 365–397. Weinheim: Wiley-VCH.

Santschi PH and Honeyman BD (1991) Radioisotopes as tracers for the interactions between trace elements, colloids and particles in natural waters. In: Vernet J-P (ed.) *Trace Metals in the Environment 1. Heavy Metals in the Environment*, pp. 229–246. Amsterdam: Elsevier.